Using zebrafish to characterise the role of LMX1b in skeletal and neuronal development, and how autophagy could participate in these processes.

Elizabeth Blyth

The author would like to acknowledge Joanna Moss (PHD student Hammond Lab) for zebrafish line creation and maintenance, conducting wet-lab experiments, and for support throughout this project. Additionally, the author thanks Dr Chrissy Hammond (project supervisor) for continued advice and support, and all members of the Hammond Lab.

ABSTRACT

The role of LIM homeobox Transcription Factor 1-Beta (LMX1b) in skeletal, ocular and neuronal patterning is well-established. More recently, LMX1b has been implicated in the regulation of autophagy, which underlies cellular differentiation, maintenance, and survival. Nevertheless, the combined and wide-ranging effects of LMX1b across all developing body systems, and underlying cellular mechanisms, remain poorly defined. Therefore, this project aimed to broadly characterise gross phenotypic changes seen in LMX1b-ablated embryonic development, using CRISPR knockout zebrafish lines of paralogues LMX1ba and LMX1bb as a model. Larval morphological assessment revealed abnormal neuronal patterning in mutants and striking discrepancies between paralogue lines. LMX1ba mutants displayed defective jaw cartilage development and stunted growth, whereas LMX1bb mutants were severely affected with oedema, uninflated swim bladders and premature death. Fascinatingly, LMX1bb mutant adults also demonstrated abnormally anxiolytic behaviour in novel environment tests. These results suggest defective LMX1b-dependent neurodevelopment might translate into abnormal adult alarm behaviour. Furthermore, phenotypes of reduced larval growth, swim bladder uninflation and oedema suggest the involvement of LMX1b-dependent autophagy in embryonic development, as autophagy impairments previously have been linked to these phenotypes. Further studies must determine the extent to which autophagy underpins LMX1b's role in early development, and additionally characterise the neuronal and adult behaviour changes we preliminarily observed in mutants. Taken together, this field aids understanding of the role LMX1b might play in human skeletal and neuronal diseases.

INTRODUCTION

The LIM Homeobox Transcription Factor 1-Beta (LMX1b) gene encodes a transcription factor that is predominantly expressed during embryonic development. Well-characterised roles of LMX1b are documented in the early patterning of the dorsoventral axis, the glomerular epithelium in the kidney and the anterior segment of the eye (Dai 2009). Interest arose in LMX1b when these specific regions were linked with the rare skeletal disease Nail Patella Syndrome (NPS), which causes malformed kneecaps and nails, nephropathy and increased glaucoma risk (Dreyer 1998, Lichter 1997). Following linkage analysis (McIntosh 1997), subsequent patient sequencing confirmed that various LMX1b heterozygous mutations result in NPS (Dreyer 1998), and single-nucleotide polymorphisms (SNPs) for LMX1b have also now been identified in glaucoma (Shiga 2018) and isolated kidney disease (Boyer 2013).

LMX1b is a member of the homeobox gene superfamily. These genes all contain a highly conserved homeobox domain and have wide-ranging functions in cellular differentiation and morphogenesis (Mark 1997). LMX1b additionally contains two zinc-finger binding domains, called LIM domains, which serve as binding interfaces for multiple proteins/cofactors to form transcription factor complexes (Matthews 2003). LMX1b also binds A/T-rich sequences (termed FLAT-elements) in promoter gene sequences to upregulate a wide range of tissue-specific transcription events in development, for instance NURR1 (in dopaminergic neurone development) and Eng-1 (in dorsoventral patterning) (Moreno 2020, Chen 2002).

LIM-homeobox genes have a highly conserved function in early neuronal patterning (Hobert 2000). LMX1b is highly expressed at the neural tube constriction known as the isthmus, which marks the boundary between the developing midbrain and hindbrain (Adams 2000). LMX1b regulates signalling cascades promoting the isthmus to secrete factors Fgf8 and Wnt1, which map the developing midbrain and hindbrain (Guo 2007). Wnt1 signalling also promotes the differentiation of mesodiencephalic dopaminergic neurones in the ventral midbrain (Anderegg 2013), and therefore specification and proliferation of these neurones is reliant on LMX1b signalling (Doucet-Beaupré 2015).

More recently, research has started implicating LMX1b in the cellular process of macroautophagy (Laguna 2015). Bioinformatics approaches demonstrate LMX1b binds FLAT-elements in multiple autophagy gene promoters to upregulate their expression, including LC3 and ATG13 (Moreno 2020). Macroautophagy, hereafter termed autophagy, involves packaging of cytoplasmic components into autophagosome vesicles, which are then degraded following fusion with lysosomes (Jeon 2017). Autophagy was previously thought to simply underpin cellular protein and waste metabolism (Dikic 2018), but is now considered a tightly

regulated, ubiquitous cellular process which promotes cellular differentiation, homeostasis, metabolism and cartilage/bone secretion (Moss 2020). It remains uncertain which LMX1b-dependent embryonic processes are mediated via upregulation of autophagy rather than non-autophagy related pathways. Therefore, in order to investigate LMX1b's wide-ranging roles in embryonic development and the underlying cellular mechanisms, a gross morphological assessment of all body systems is primarily required.

Zebrafish are an optimum model for this purpose. Although they have a different evolutionary lineage to mammals and therefore translatability is poorer than with a mammalian model organism, zebrafish still offer many advantages for neuronal and skeletal study. External fertilisation and transparency of embryos enables excellent visualisation of early development (Kimmel 1995). Additionally, high genetic tractability enables transgenic reporter and CRISPR/Cas9 knockout lines to be created more easily than in mammalian species (Fontana 2018). Zebrafish skeletal system development is similar to that in mammals, and the zebrafish lower jaw is particularly comparable with mammalian endochondral ossification (Mork 2015). Zebrafish neurological development is also homologous to other vertebrates, so zebrafish are commonly used to study experimental manipulations in neurogenesis (Schmidt 2013). Moreover, adult zebrafish are effective models of neurodegenerative diseases such Parkinson's Disease (PD), where assessing dopaminergic neurone survival following MPTP-injection is common (Khuansuwan 2019). Additionally, the profile of autophagy proteins is highly conserved between zebrafish and mammals (Moss 2020).

Zebrafish lineage experienced a genome duplication unseen in mammalian evolution (Postlethwait 1998). This extra polyploidisation step means zebrafish commonly express two paralogues of the corresponding mammalian gene. The mammalian orthologue LMX1b corresponds to two zebrafish paralogues, termed LMX1ba and LMX1bb (O'Hara 2015). Therefore, LMX1ba and LMX1bb knockout lines must be created separately, before crossing into a double LXM1ba/LMX1bb knockout zebrafish line. This project analysed single knockout lines in larvae, however due to the availability of data, double knockout lines were included in adult analysis.

METHODS AND MATERIALS

All experiments were conducted following ethical approval from the Home Office and in accordance with COSHH safety guidelines. Wildtype and mutant larvae were kept in Danieu solution until 5dpf before transfer to the Zebrafish Facility and were maintained under standard conditions (Aleström 2020). Due to COVID-19 Pandemic restrictions, Joanna Moss (PHD student) conducted in-person lab experiments and uploaded images online for this analysis.

Creating CRISPR knockout lines

Separate CRISPR zebrafish LMX1ba and LMX1bb knockout lines were created, as shown in Fig.1. Selected gRNA sequences were injected at single-cell stage, and subsequent fragment analysis of larval DNA revealed the most effective gRNA larvae population. These generation zero (G0) mosaic mutants were outcrossed with wildtype. Crossing the resulting G1 heterozygotes produced Mendelian ratios of G2 heterozygote (het), homozygote (homo) and wildtype (wt) larvae. These were genotyped using Sanger Sequencing. G2 homozygotes were crossed to produce stable homozygous mutant (termed homoinX) lines of LMX1ba. LMX1bb homozygotes (LMX1bb-/-) die as juveniles. Therefore, LMX1bb knockout lines were maintained in their heterozygous state (hetinX).

Analysis involved assessing offspring from LMX1ba homoinX, LMX1ba hetinX and LMX1bb hetinX lines. Whole embryo post-mortem genotyping of hetinX larvae occurred on 7dpf. HetinX larvae were therefore analysed double-blind, with genotype revealed post-analysis.

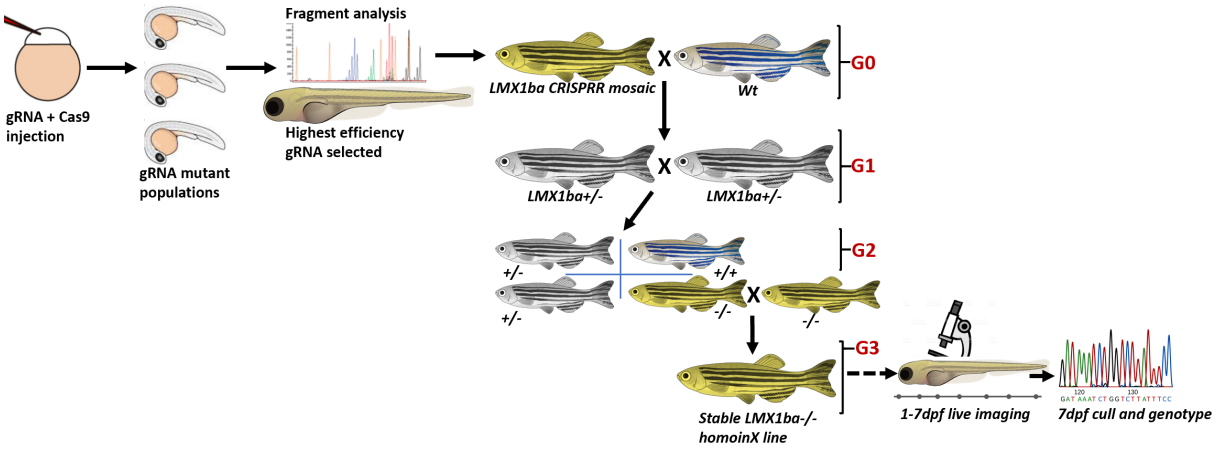

Figure 1 *Schematic depicting generation of LMX1ba knockout line and imaging of larvae. Identical protocol generated LMX1bb mutants.*

Bioinformatics

Multisequence alignment (MSA) of protein sequences was performed using EMBL-EBI Clustal Omega tool (Madeira 2019) to compare percentage similarity between amino acid sequences (see Fig.2). Protein sequences of LIM1, LIM2 and Homeobox domains were individually aligned using UniProt BLAST tool (UniProt 2021). Transcript and protein sequences were obtained from the NCBI database (NCBI 2021).

NCBI wildtype LMX1ba/bb sequences were aligned against experimental mutant transcripts using Snapgene (Snapgene-Software 2021). The CRISPR-induced indel mutation sites were

located (see Fig.3A). These mutations were manually introduced into wildtype LMX1ba/bb sequences (Fig.3B), and the resulting protein sequences were assessed (Fig.3C).

Gross morphological assessment of larvae

Live imaging of anaesthetised larvae was performed every 24 hours until 7dpf, using brightfield stereomicroscopy at 1-8.3xmagnification. 4dpf was not recorded. Where possible, images were taken from the lateral aspect. Scales were calibrated on ImageJ (Schindelin 2012).

Images were qualitatively assessed for the following gross morphological phenotypes: oedema, swim bladder inflation, yolk sac, eye oedema, upper spinal bend (which are markers of early zebrafish development) and kidney cysts, eye oedema, and tail bends (body parts relevant to LMX1b expression). Body length and eye diameter were measured manually with the segmented line tool on ImageJ. Body length is a larval developmental marker and eyes are investigated due to LMX1b high expression here.

Oedema was classified as no/mild/severe (see Fig.6B), in accordance with existing literature (Shin 2016). For analysis, larvae were allocated oedema phenotypes in their 7dpf image or final image before death. Larvae were characterised as ‘uninflated swim bladder’ when swim bladder did not inflate at any dpf. Partial inflation was recorded as full inflation because this is observed normally.

Body length was measured from snout, to centre of eye, to otolith, to first somite, then tracking the notochord until the caudal peduncle (shown in Fig.5A,B). This technique ensured that body length was not confounded by spinal curvatures (Kimmel 1995).

Eye diameter was manually measured as the longest visible diameter of the eye (Parichy 2009) (see Fig.5A,B). Where eyes overlapped on a non-lateral image, the diameter of a single eye was estimated.

Morphological assessment of adult zebrafish

Lateral images were taken of anaesthetised fish (aged 6.5-7.5mpf) using a camera. Following scale calibration, body length and eye diameter were measured following previously-stated methods (shown in Fig.5C).

Quantifying lower jaw length and Sox9a expression

Culled 3dpf and 5dpf larvae were fixed for whole-mount immunohistochemistry following standard procedure (Westerfield 2007). The prepared larvae were treated with anti-col2a and anti-Sox9a antibodies followed by fluorophore-labelled anti-rabbit and anti-mouse secondary

antibodies. Confocal microscopy was performed from the ventral aspect, and Maximum Projection images were assembled on ImageJ.

The ImageJ line tool was used to manually measure full lower jaw length, and width and length of Meckel's cartilage, shown in Fig.7A.

Confocal Z-stack images were imported into Seg3D, a purpose-built extension of Matlab (Seg3D 2016). The volume of Sox9a staining contained within a manually-drawn region of interest in the Z-stack provided a readout of Sox9a intensity (see Fig.7B).

Preliminary neuronal immunohistochemistry

Small samples of LMX1ba-/-, LMX1bb-/- and wildtypes were culled on 1-7dpf. Whole-mount acetylated tubulin (ACT) and tyrosine hydroxylase (TH) immunostaining as well as DAPI staining was conducted. Images of the head region were collected from various angles using confocal microscopy.

The only directly comparable images were 5dpf dorsal images of LMX1bb-/- and wildtype TH-stained larvae. Gross patterns of TH-staining were qualitatively assessed from confocal Z-stack projections on ImageJ (see Fig.8A).

Preliminary morphological assessment of midbrain-hindbrain boundary (MHB)

1dpf larval brightfield images were selected which contained overlapping eyes and a non-blurry head outline. This is necessary because the MHB is best visualised on high-quality lateral images (Vaz 2019). Larvae were allocated to the following categories (see Fig.8B) based on existing literature (Jászai 2003):

'Normal MHB': visible midbrain, hindbrain and developing cerebellum (termed cerebellar anlage).
'Moderate MHB abnormality': caudal enlargement of the tectum (part of midbrain), absent cerebellar anlage.
'Severe MHB abnormality': no distinct boundaries present in midbrain/hindbrain/cerebellar region.

Assessing adult alarm behaviour

Novel environment behavioural tests were conducted on 6.5mpf LMX1ba-/-, 7mpf LMX1bb+/-, 7mpf LMX1ba;LMX1bb+/- (double heterozygous knockout) and 7.5mpf wildtype zebrafish, using protocol devised from Formella 2012. Surrounding noise was minimised. Zebrafish were individually placed into novel tanks and video-recorded for 10 minutes. Number of seconds of 'bottom-dwelling' behaviour (fish occupying base of the tank) and freezing behaviour

(immobile at base of tank) was recorded in the 1st and 10th minute, using a manual stopwatch (see Fig.9A).

Statistical Methods

Normality was assessed with D'Agnostino Pearson and Shapiro-Wilks Tests on Prism (GraphPad Prism V9.0) for each data set. All normality tests were passed thus parametric tests were performed.

LMX1ba and LMX1bb hetinx yielded separate wildtype and heterozygote data, which was initially compared using Prism multiple comparisons tests. When LMX1ba and LMX1bb wt and het samples were not significantly different they were combined into a 'siblings' (sibs) group, and sibs were analysed against homo mutants. For body length, LMX1ba sibs were significantly different from LMX1bb sibs, so each mutant paralogue was analysed against their corresponding sib group.

Prism unpaired t-tests were performed to compare differences in mean body/eye/jaw lengths, Sox9a volumes and bottom-dwelling/freezing times. Prism 2-way ANOVA and Tukey Multiple Comparisons were used to analyse body/eye lengths over 1-7dpf.

Freeman-Halton Tests were conducted for categorical data (swim bladder inflation, oedema and MHB phenotypes) using VasaarStats online tool (Lowry 2021). This is an extension of Fisher's Exact Test for 3x2 matrices. This frequency-based analysis was chosen to account for highly variable sample sizes between genotype groups.

Post-hoc power analysis of Sox9a volume data was conducted using ClinCalc online tool (Kane 2021).

Graphical data was created on Prism; error bars represent 95% confidence intervals.

RESULTS

Bioinformatics reveals high conservation between Danio Rerio and Homosapiens LMX1b

The high protein sequence similarity seen pictorially between *Danio Rerio* (zebrafish) paralogues and *Homosapiens* LMX1b in Fig.2B is confirmed by high MSA percentage similarity in the whole protein and domain sequences (shown in figure 1 and 2). The LMX1b protein is 100% conserved between Mus Muscularis (common mouse) and humans (see figure 1 and 2). Zebrafish LMX1bb displays higher % similarity to *Homosapiens* than LMX1ba in LIM1 and LIM2 domains, however the Homeobox domain is identical across all species.

High conservation across vertebrates gives confidence that LMX1b protein function is also likely similar.

CRISPR-induced LMX1ba and LMX1bb indel mutations cause frame-shifts (see Fig.3B), premature stop codons and hence truncated protein (see Fig.3C).

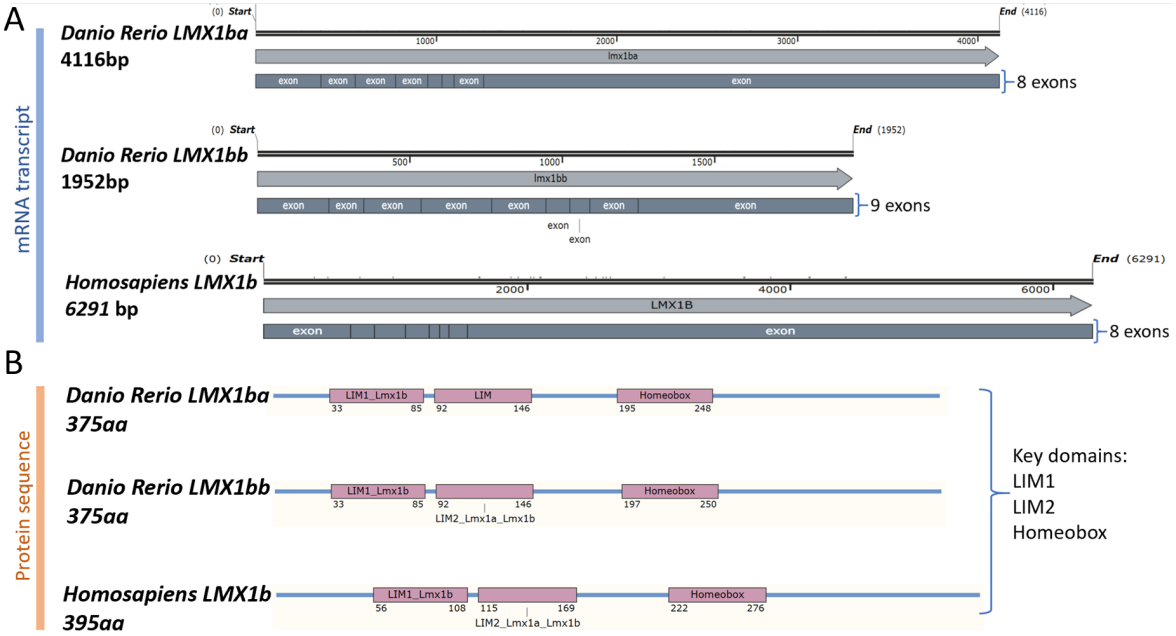

Figure 2 *Schematic illustrating transcript (A) and protein (B) sequences for Homosapiens LMX1b and zebrafish paralogues including sequence lengths, exon number and key domains, showing high conservation of LMX1b protein domains.*

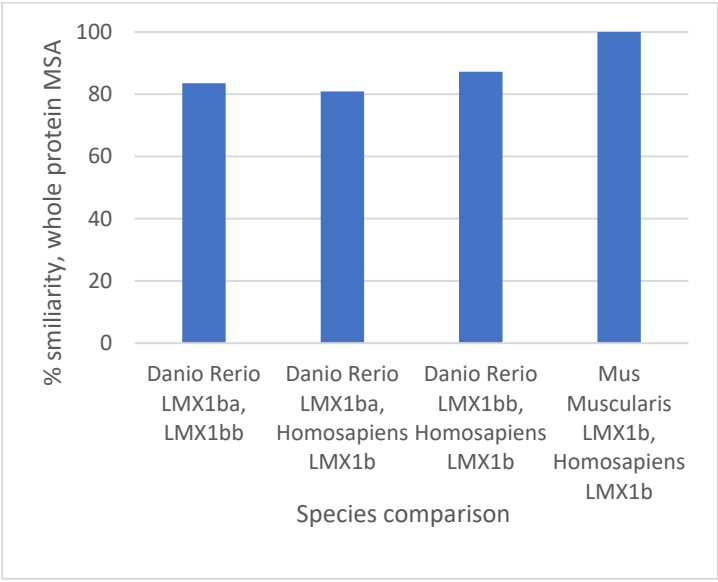

Figure 1 *Percentage Similarity for LMX1b Danio Rerio, Homosapiens and Mus Muscularis indicates high protein % similarity between zebrafish paralogues and mammalian LMX1b.*

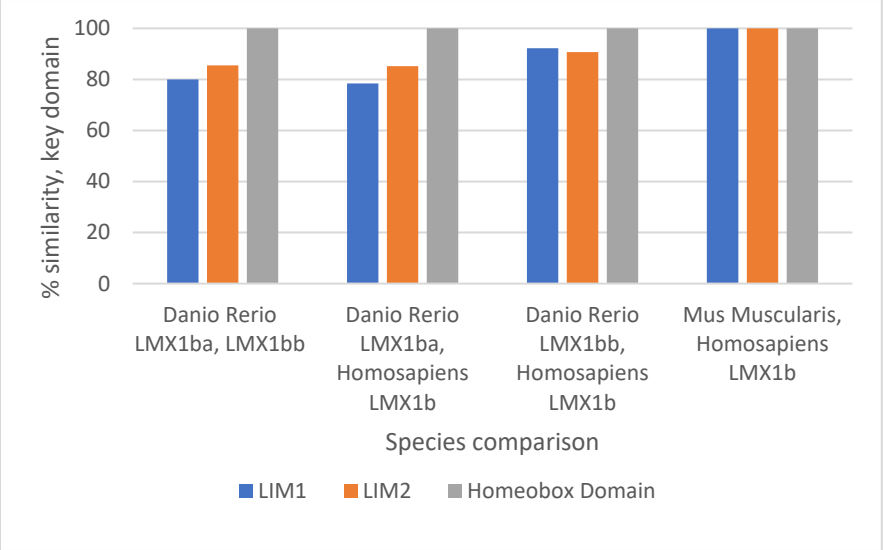

Figure 2 *Percentage Similarity for key LMX1b domains in Danio Rerio, Homosapiens and Mus Muscularis indicates high conservation of domain sequences between zebrafish paralogues and mammalian LMX1b.*

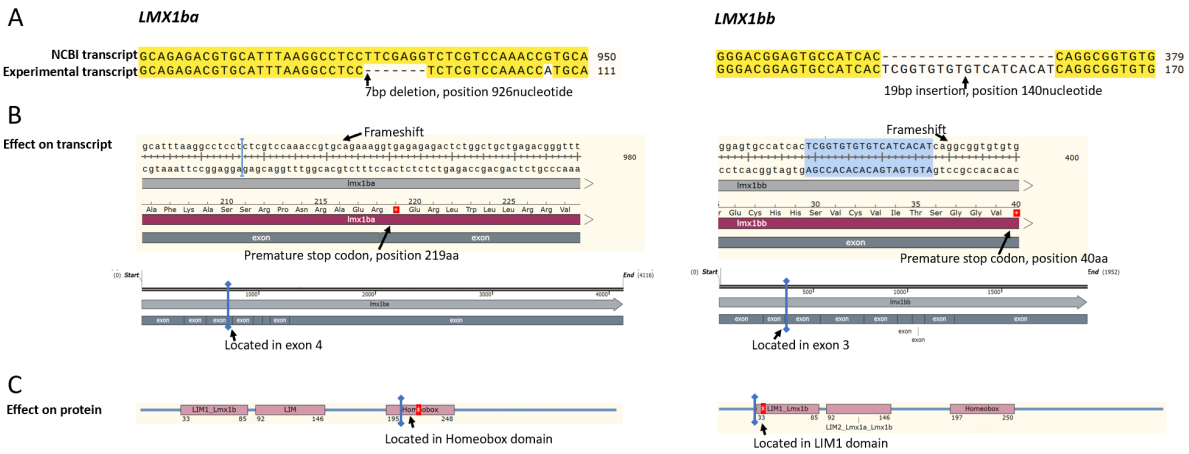

Figure 3 *Schematic displaying mutation sites in experimental LMX1ba and LMX1bb transcripts (A), resulting premature stop codons in transcript (B) sequences and truncated protein (C) sequences, indicating null mutants.*

LMX1ba-/- and LMX1bb-/- mutants show markedly different abnormal phenotypes in development

Gross morphological assessment was conducted to identify developmental abnormalities in mutants. Both mutants displayed MHB abnormalities at 1dpf. Only LMX1bb-/- developed a

severe phenotype of oedema and uninflated swim bladders from 5dpf, and died before adulthood.

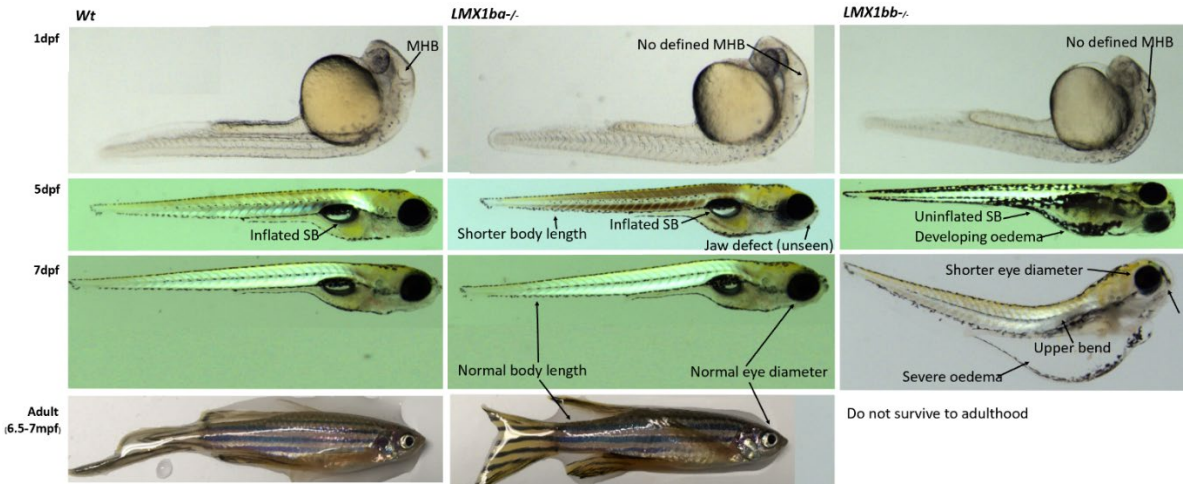

Figure 4 *Characteristic phenotypes in mutant and wildtype zebrafish through development. Abnormal MHB brain morphology, shorter body length and eye diameter, oedema and swim bladder uninflation are observed in mutants.*

Decreased body length is seen in LMX1ba-/- and decreased eye diameter in LMX1bb-/- larvae

As shown in Fig.5D, comparisons of mutant and wt larvae reveal LMX1ba-/- are significantly shorter than corresponding sibs at 3dpf (212μm±124 shorter) and 5dpf (153.8μm±143 shorter). Interestingly, the shorter body length is not maintained in LMX1ba-/- beyond 5dpf, and is not seen in LMX1ba-/- adults (see Fig.5G). In contrast, LMX1bb-/- larvae are not significantly different in length to the corresponding sib population. These results surprisingly suggest that LMX1bb+/- adults are significantly longer than wt (mean difference -3656μm±1599) (see Fig.5G). Tank and feeding conditions of wt and mutant fish lines must be controlled in order to confirm this finding and rule out the possibility of stock density issues confounding results.

As shown in Fig.5F, LMX1bb-/- larvae display significantly reduced eye diameter compared to sibs from 5dpf onwards (mean difference at 5dpf -24.21μm±18.729, 6dpf -43.64μm±26.55, 7dpf -38.51μm±19.53), which is not replicated in LMX1ba-/- larvae or adult populations.

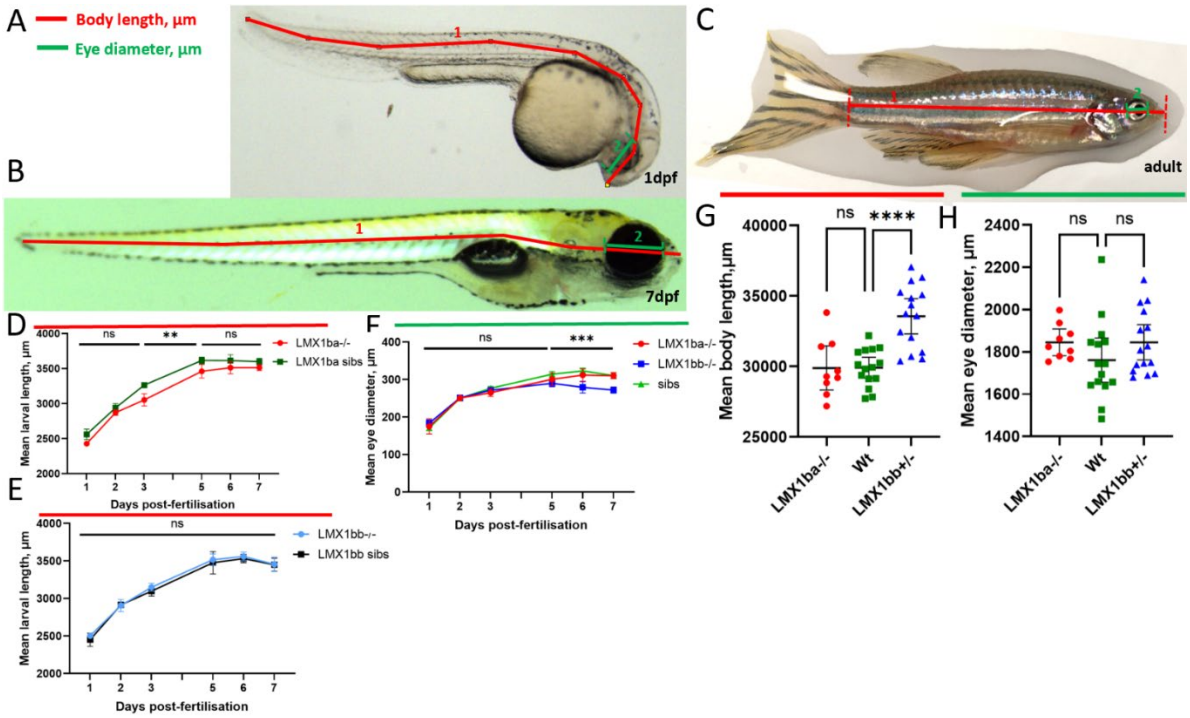

Figure 5 *(A,B,C) Schematics showing body length and eye diameter measurements in 1dpf larvae, 7dpf larvae and adult zebrafish respectively. (D) Graph showing significantly shorter body length of LMX1ba-/- vs LMX1ba sibs at 3-5dpf (3dpf p<0.0001, 5dpf p=0.031, Tukey's multiple comparisons, 2-way ANOVA) (n≥32). (E) Same as (D) for LMX1bb-/- and sibs, where no difference is observed (n≥19). (F) Graph depicting significantly reduced mean eye diameter of LMX1bb-/- vs sibs at 5-7dpf, with no difference in LMX1ba-/- vs sibs (LMX1bb-/- vs sibs 5dpf p=0.007, 6dpf p=0.0004, 7dpf p<0.0001, Tukey's multiple comparisons, 2-way ANOVA). (G) Graph indicating significantly increased mean body lengths of 7mpf LMX1bb-/- vs 7.5 mpf sibs and 6.5mpf LMX1ba-/- and 7mpf wt (LMX1bb+/- vs wt* p<0.0001, unpaired t-test) *(n≥9). (H) Same as (G) for eye diameter, with no difference between mutants vs sibs.*

Uninflated swim bladders and development of severe oedema in LMX1bb-/- larvae

Striking differential penetrance of oedema and swim bladder phenotypes is observed between mutant and sib larvae (see Fig.6C,D). Whilst the majority of LMX1bb-/- had uninflated swim bladders (16 out of 19 larvae) and severe oedema (all 19 larvae) by 7dpf, het were not significantly different from wt suggesting a recessive pattern of inheritance. These phenotypes were not evident in LMX1ba-/-.

The generalised oedema is accompanied by eye oedema (see Supp.Fig.2), and typically first presented at 5/6dpf. Lymphoedema cannot be the sole contributor due to the zebrafish lymphatic system being undeveloped at 5dpf (Jung 2017), however the observed phenotype is not typical of isolated renal-induced/cardiovascular oedema (this onsets prior to 5dpf, often

with pronounced pericardial oedema, Cosentino 2010). Therefore, a combination of lymphoedema with renal-induced/cardiovascular oedema is suspected.

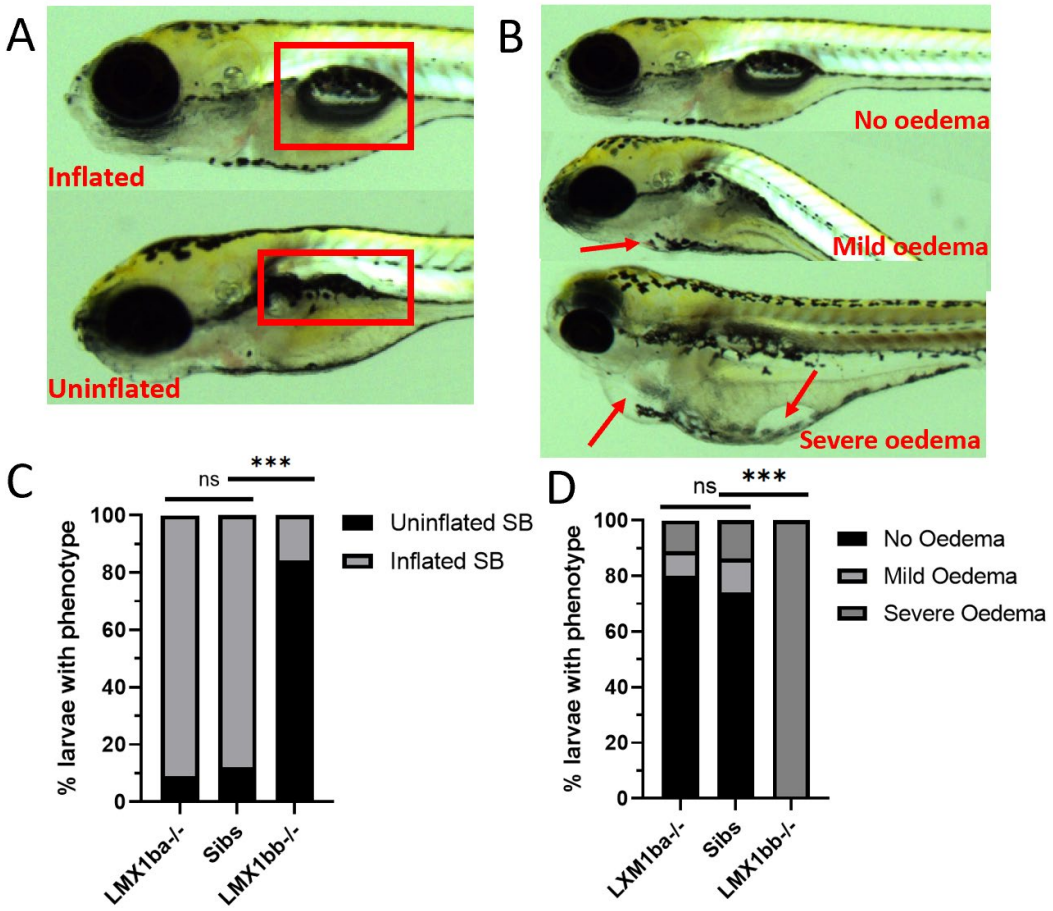

Figure 6 *(A) Appearance of inflated and uninflated swim bladder larval phenotypes. (B) Representative examples of no/mild/severe oedema classification system. (C) Graph indicating 84% LMX1bb-/- larvae display uninflated swim bladders but no difference between sibs and LMX1ba-/-. (LMX1bb-/- vs sibs p<0.0001, Freeman-Halton Test) (n≥19). (D) Graph showing proportion of mutants and sibs with oedema phenotypes, with 100% LMX1bb-/- displaying severe oedema and no significant difference between LMX1ba-/- vs sibs (p<0.0001, Freeman-Halton Test) (n≥19).*

LMX1ba-/- show decreased lower jaw dimensions at 3 and 5dpf

Immunostaining for Col2a (the primary component of developing cartilage matrix) enabled visualisation of the cartilage template and jaw outline (Gistelinck 2016). As shown in Fig.7I-K, LMX1ba-/- but not LMX1bb-/- displayed significantly shorter full lower jaw and Meckel's cartilage lengths (-30.24µm±21.44, -27.05µm±8.88 respectively). Following this finding, 3dpf LMX1ba-/- larvae were investigated, and significantly decreased full length was also observed at this younger age (-27.08µm±24.568) (see Fig.7D-F). There was no difference between 3-

5dpf percentage growth of LMX1ba-/- and wt lower jaws (see Supp.Fig.3), indicating that LMX1ba's effect on jaw growth occurs predominantly before 3dpf. Qualitative examination suggested that 3dpf LMX1ba-/- jaw outlines were more uneven than wt.

Noticeable decrease in larval lower jaw Sox9a expression is not quantitatively significant

Immunostaining for Sox9a (a transcription factor promoting chondrocyte differentiation) served as a proxy for chondrocyte maturation and health (Yan 2002). Qualitative assessment of confocal images suggested Sox9a expression was reduced in 3dpf and 5dpf LMX1ba-/-. However, subsequent quantitative analysis did not reveal significant differences in Sox9a intensity compared to wt, despite pronounced differences in mutant and wt mean intensity readings (mean difference LMX1ba-/- vs wt 3dpf $-2.03 \times 10^5 \mu m^3 \pm 3.11 \times 10^5$, 5dpf $-3.08 \times 10^5 \mu m^3 \pm 3.21 \times 10^5$, LMX1bb-/- vs wt $-1.94 \times 10^5 \mu m^3 \pm 3.10 \times 10^5$) (see Fig.7G,L). Post-hoc power analysis demonstrated that wide variation in intensity readouts, particularly in wildtypes, resulted in extremely low power of 44%. Obtaining 80% power would require n=52 (Kane 2021).

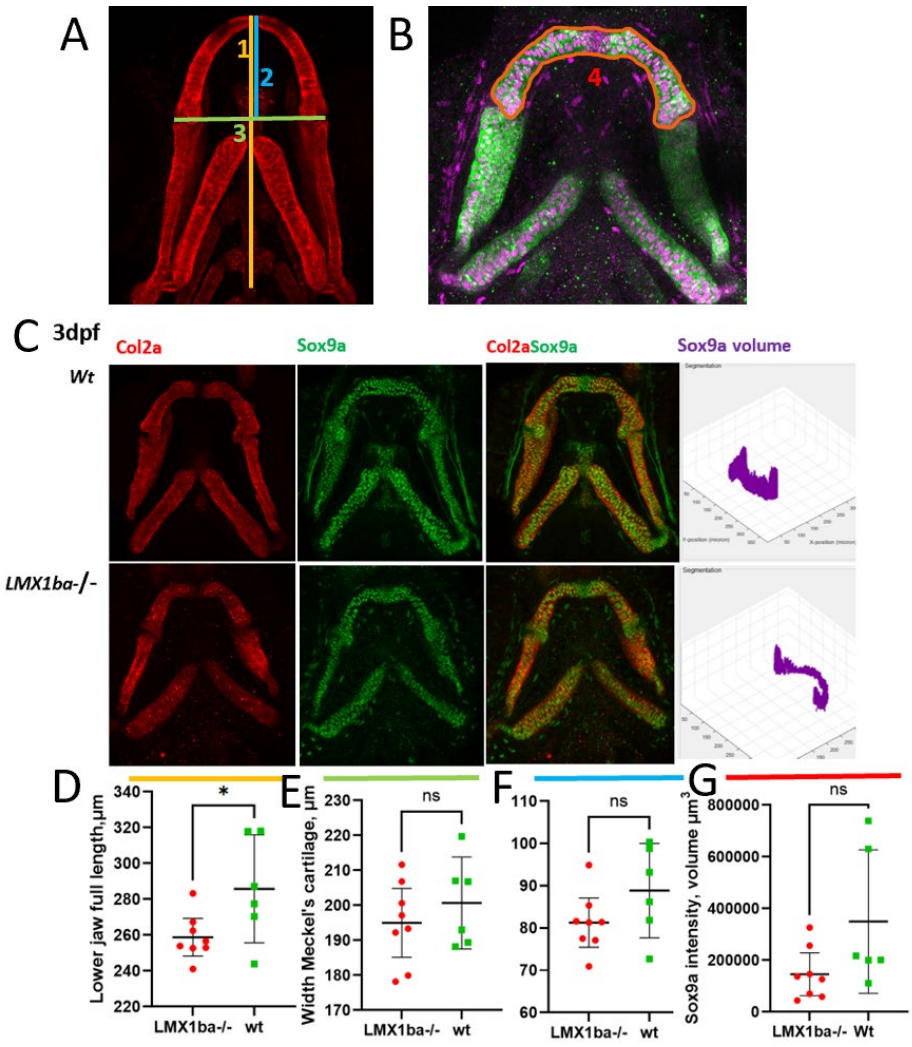

Fig.7 continues overleaf.

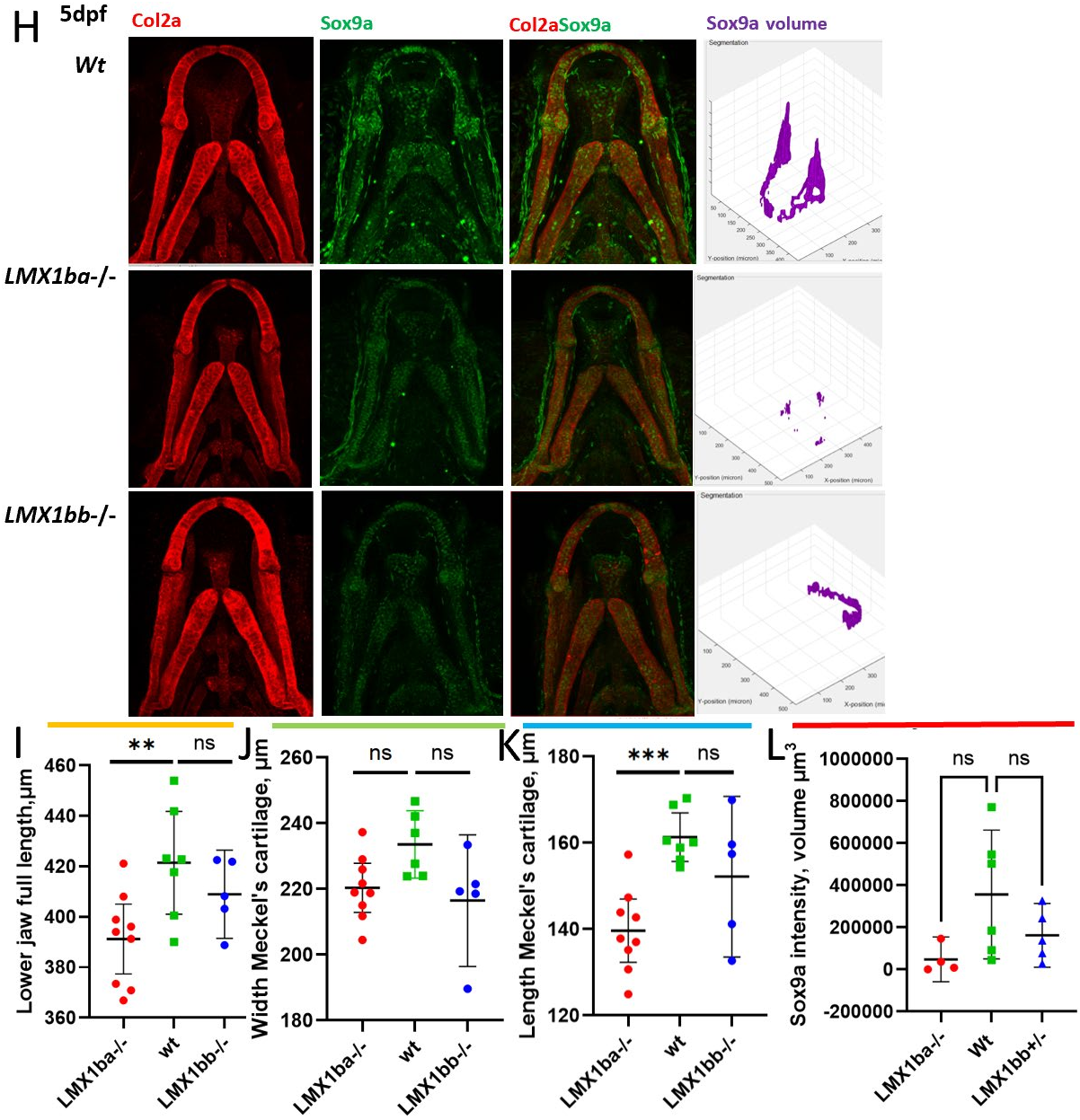

Figure 7 *(A) Schematic illustrating lower jaw length measurements from ventral-view Col2a Z-stack projections (1=full lower jaw length, 2=length Meckel's cartilage, 3= width Meckel's cartilage). (B) Example of manually-drawn ROI on Seg3D (4=ROI encompassing entire Meckel's cartilage). (C) Representative examples of 3dpf LMX1ba-/- and wt jaw images, illustrating reduced Sox9a volume and smaller jaw dimensions in LMX1ba-/- mutants. Col2a, Sox9a and merged Col2aSox9a confocal images are Max Z-stack projection images of Col2a/Sox9a immunostaining. Sox9a volume images are 3D models of Sox9a intensity output on Seg3D programme. (D-F) Graphs comparing mean jaw lengths in 3dpf LMX1ba-/- and wt larvae, indicating LMX1ba-/- have significantly smaller full lower jaw length but other dimensions are similar (full length p=0.0336, unpaired t-test) (n≥6). (G) Graph indicating the reduced Sox9a volume intensity readout in 3dpf Meckel's cartilage in LMX1ba-/- is*

nonsignificant vs wt (n≥6).(H) Same as (C) for 5dpf. (I-K) Same as (D-F) for 5dpf mutant and wt larvae, indicating LMX1ba-/- have significantly reduced lower jaw full length and Meckel's length vs wt and LXM1bb-/- (LMX1ba-/- vs wt full length p=0.0129, width Meckel's p=0.0013, unpaired t-test) (n≥6). (L) Same as (G) for 5dpf larvae (n≥4), indicating the reduction Sox9a intensity in mutants is nonsignificant.

Mutants display altered patterning of TH-positive neurones and MHB

Qualitative assessment of TH-staining, which labels catecholamine-positive neurones (predominantly dopamine and noradrenaline, Filippi 2010) reveals lack of TH-positive cell organisation in the LMX1bb-/- gross forebrain/midbrain region (shown in Fig.8A). This potentially indicates compromised dopaminergic neurone development (Filippi 2010).

Shown in Fig.8C, assessment of MHB appearance in 1dpf larvae brightfield images revealed significantly higher incidence of MHB abnormality in both LMX1ba-/- and LMX1bb-/- than sibs (p=0.0121, p=0.0228, Freeman-Halton Test). MHB abnormalities were most prevalent in LMX1b-/- larvae, presenting in 8 out of 12 LMX1bb-/- larvae.

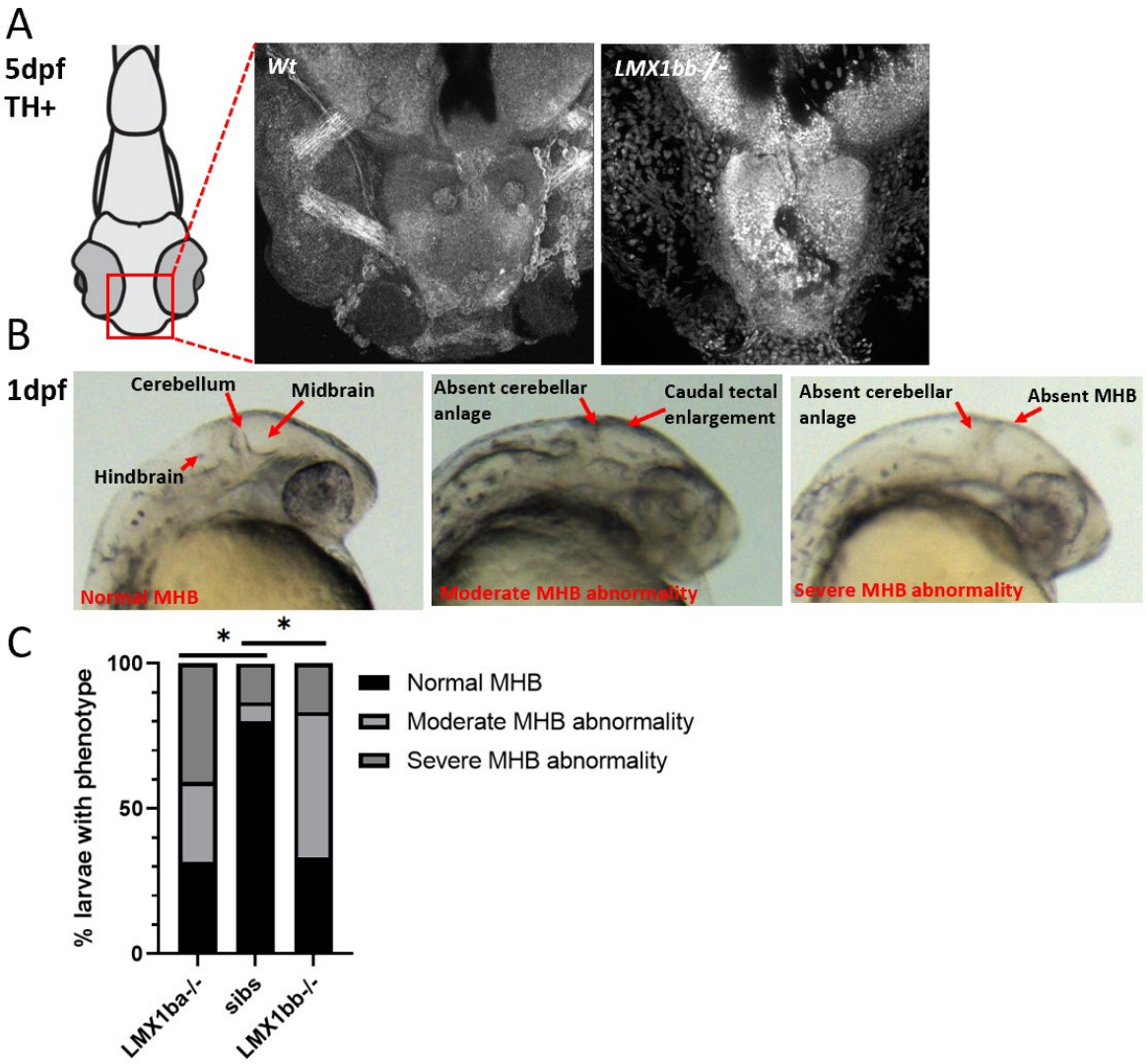

Figure 8 *(A) Example of dorsal-view TH-stained confocal images of 5dpf LMX1bb-/- and wt brains. No LMX1ba-/- images were available. (B) Appearance of normal/mild/severe MHB abnormality classification in 1dpf brightfield lateral-view images. (C) Graph indicating a higher proportion of mutants display MHB abnormalities compared to sibs (n≥12).*

LMX1bb-/- and LMX1ba;LMX1bb+/- adults showed diminished alarm behaviour in novel environment tests

When placed in a novel environment, zebrafish normally exhibit increased bottom-dwelling and freezing behaviour in order to 'hide' from predators (Kalueff 2013, Sackerman 2010). As seen in Fig.9B/C, LMX1bb+/- and LMX1ba;LMX1bb+/- demonstrated impaired bottom-dwelling behaviour that was significant in 1st min (-52.07%±35.54, -46.23%±35.55 respectively). Freezing behaviour was non-existent in 1st min, however 3 of the 4 wt and LMX1ba-/- adults froze for a large proportion of 10th min, compared to none of the LMX1bb+/- or LMX1ba;LMX1bb+/- (see Fig.9D). Behaviour of LMX1ba-/- was indistinguishable from

wildtype. The differential behaviours of LMX1ba and LMX1bb mutants suggests two alleles of LMX1bb are required for normal alarm behaviour.

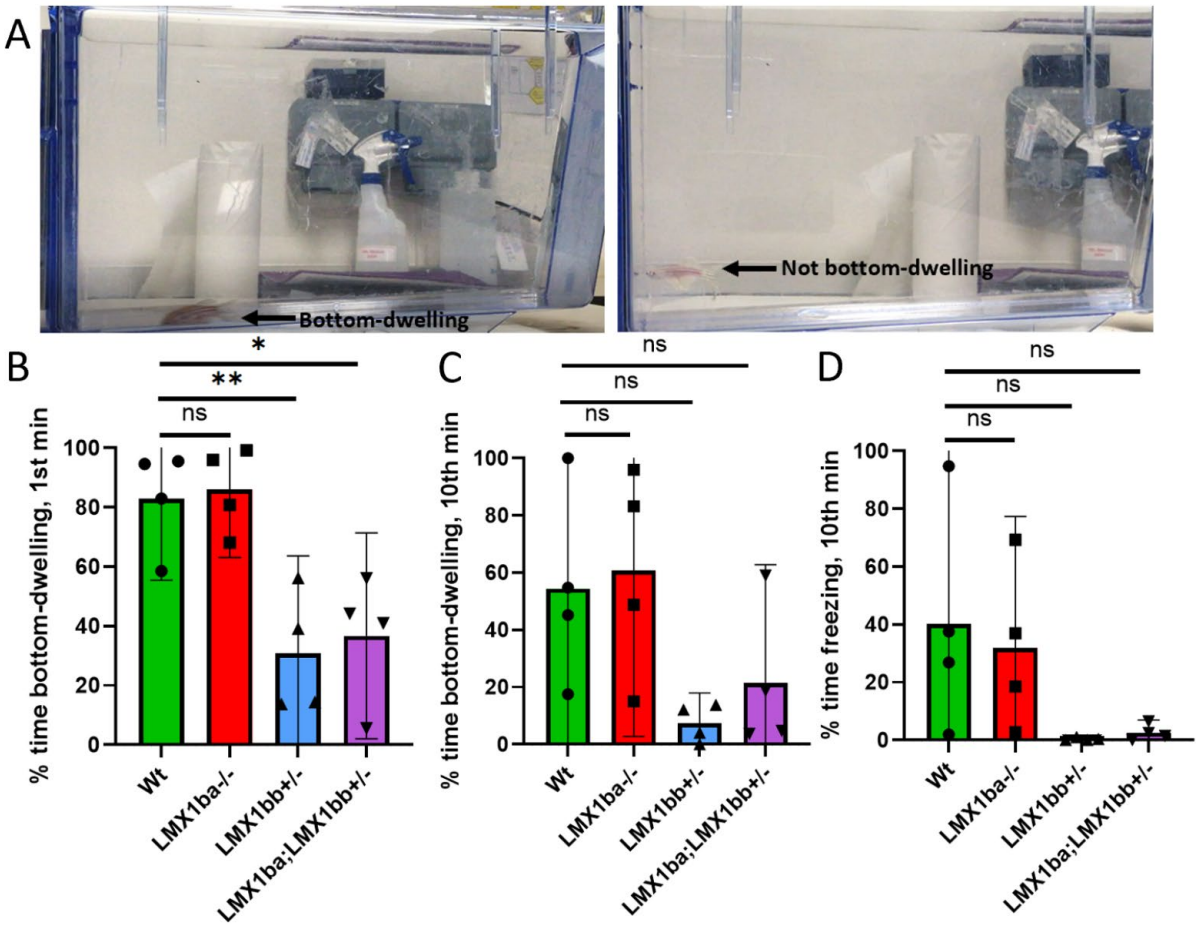

Figure 9 *(A) Examples of bottom-dwelling and non-bottom dwelling behaviour. (B) Graph of % time adult zebrafish spent bottom-dwelling during 1st minute indicating LMX1bb heterozygous mutants spend significantly less time dwelling at the bottom (LMX1bb+/- vs wt p=0.0053, LMX1ba;LMX1bb+/- vs wt p=0.0117, unpaired t-tests) (C) Same for (B) for 10th min, showing the apparent reduction in bottom dwelling time in LMX1bb heterozygous mutants is nonsignificant (D) Graph illustrating the % reduction in freezing time in 10th min in mutants is nonsignficant (n=4 for all).*

DISCUSSION

These results highlight a striking role for LMX1b in multiple aspects of zebrafish larval development. This discussion principally focusses on differential morphologies, underlying autophagy processes and neurodevelopmental implications, with the inclusion of experimental shortcomings and model suitability.

Significance of broad morphological changes

LMX1b mutations presenting in human patients are only found in heterozygous form, and result in specific non-lethal patterning defects of the dorsoventral axis and eyes (Witzgall 2017) with no evident neurodevelopment/autophagy changes. The broader phenotypic changes seen in our zebrafish indicate that LMX1b homozygous knockout might impair embryonic autophagy and neurodevelopmental processes, and it is therefore possible that similar autophagy/neuronal defects might be causing the prenatal death of human LMX1b homozygous mutants.

The location of mutations seen in Bioinformatics analysis (Fig.3) indicates that both LMX1ba and LMX1bb mutants are null. Our results also suggest differential paralogue expression. LMX1bb-/- are the more severely affected mutant, displaying uninflated swim bladders and oedema post-5dpf which culminates in premature death. Specifically, the milder-affected LMX1ba-/- show shortened body length and jaw cartilage abnormalities, suggesting selective LMX1ba expression in the jaw. 20% of LMX1ba-/- larvae also display an inconsistently penetrant lethal phenotype at 2dpf (see survival analysis, Supp.Fig.1). Finally, preliminary analysis indicates that in LMX1bb, but not LMX1ba mutants, neurodevelopmental abnormalities may translate into impairment of certain adult behavioural responses. The differential spatial expression of LMX1ba/bb could be confirmed through FACS-sorting specific cell populations, for instance larval chondrocytes (Manoli 2012).

Autophagy impairment as an explanation of mutant developmental abnormalities

Defective autophagy-driven lipid metabolism and stunted growth

LMX1ba-/- show decreased body length in larval development (see Fig.5) which appears to catch up with wt by 6/7dpf. This coincides with a feeding switch. From 6dpf onwards, larvae were fed with protein (brine trim) rather than reliance on yolk sac lipids. Lipid metabolism, but not protein metabolism, has been shown to be autophagy-dependent (Singh 2009). Indeed, unpublished findings from the Hammond Lab indicate that ATG13-/- (a critical autophagy-related gene) larvae show impaired yolk sac metabolism and stunted growth (Unpublished Moss 2021). Therefore, it is postulated that LMX1ba-/- early growth is impaired due to inability to metabolise the yolk sac, whereas protein diets administered from 6dpf are metabolised as

normal. Changing larvae diets from protein to fat would illustrate whether continued inability to metabolise does decrease body length (Minchin 2018). Alternatively, reduced body length could indicate a spinal defect; reduced number of somites (seen in abnormal spinal patterning) decreases notochord length (Resende 2014). Somite number should be counted in brightfield larval images to assess for patterning defects.

Defective lymphatic vessel lipid metabolism and oedema phenotype

LMX1b's role in the autophagy pathway of lipid metabolism may also underlie the observed lymphoedema phenotype. Even though the role of LMX1b, or autophagy more generally, in lymphoedema is yet to be explored, lymphatic endothelial cells are worse affected in autophagy knockout models than other endothelial cells (O'Sullivan 2016). This is thought to be because lymphatic cells have a greater reliance on lipid droplets as a source of fatty acids for mitochondrial metabolism than other endothelial cells (Wong 2017). Autophagy assists in the degradation of lipid droplets to fatty acids, and in-vitro autophagy knockout models impair fatty acid oxidation, lipid metabolism and lymphangiogenesis (O'Sullivan 2016). However, the relative contributions of cardiovascular and renal-induced oedema to the mutant phenotype must be confirmed. Decreased LMX1b expression in renal podocytes (Rohr 2002) may result in a malformed and leaky glomerular filtration barrier (Hanke 2013) which could contribute significantly to the observed oedema.

It is postulated that reductions in eye diameter specifically in LMX1bb-/- at 5-7dpf (see Fig.5) might be explained by the associated increase in eye oedema over this time (see Supp.Fig.2). LMX1b's role in eye development, specifically in the migration of periocular mesenchymal cells (McMahon 2009), is well-characterised (Richardson 2017). Nevertheless, it is likely that increased pressure in eye oedema underlies the pronounced ocular shrinkage (Arden 2011) rather than ocular developmental defects, because eye oedema presented the fish which also had severe oedema.

Uninflated swim bladders could be explained by surfactant production deficit

LMX1bb-/- larvae additionally display uninflated swim bladders. This could substantiate evidence that autophagy is required for inflation of air-filled cavities (Morishita 2020). Research shows that autophagy impairment decreases surfactant production by lamellar bodies in mouse lungs and zebrafish swim bladders. Surfactant is required to reduce surface tension and inflate these cavities (Chen 2018), so reduced surfactant is postulated to decrease swim bladder inflation. ATG13-/- mutants with impaired autophagy also demonstrate uninflated swim bladders (Unpublished Moss 2021), suggesting our observed phenotype might also be due to defective autophagy. Taken together, these results potentially implicate LMX1bb in autophagy-mediated surfactant production.

Developmental jaw defects suggest impaired chondrocyte autophagy

Reduced jaw length and uneven template boundaries (visualised by Col2a staining) indicates defective cartilage secretion by chondrocytes specifically in LMX1ba-/-. Moreover, qualitative data suggests that LMX1ba-/-, and also perhaps LMX1bb-/-, might display reductions in Sox9a intensity. Sox9a marks chondrocytic maturation and development, and this is partially regulated by autophagy (Aghajanian 2018). Indeed, preliminary findings demonstrate that ATG13-/- mutants likewise have reduced lower jaw Sox9a expression and maldeveloped chondrocytes (Unpublished Moss 2021). Hence, these results suggest that LMX1b may be necessary for autophagy-dependent chondrocyte differentiation, to enable Col2a secretion in the developing cartilage template of the lower jaw. Alternatively, the jaw phenotype also could be due to reduction in LMX1b skeletal expression; human patients with LMX1b heterozygous mutations show skeletal deformities and the zebrafish jaw models skeletal systems.

Although the above morphological changes may result from defective autophagy-mediated LMX1b processes, non-autophagy roles of LMX1b for example in skeletal patterning and kidney patterning could also underlie changes (jaw and length phenotype and oedema phenotype respectively). Autophagy flux experiments would determine whether autophagy is defective in which locations in these mutants.

Linking neuronal patterning abnormalities and reduced alarm behaviour

Neurodevelopmental abnormalities possibly due to defective neuronal autophagy

At 1dpf, MHB patterning appears significantly altered in both mutant paralogues. The observed phenotype of abnormal tectal and cerebellar morphology is similar to previous LMX1b ablation models in zebrafish, chick and mouse embryos (O'Hara 2005, Adams 2000, Guo 2007), and confirms the crucial role of LMX1b in early patterning. Nevertheless, future whole-mount in-situ hybridisations of MHB markers such as Otx2 and Pax2a (Kesavan 2017) are required to visualise 1dpf MHB abnormalities more precisely. Preliminary observations also indicate disruption of TH-positive neurone development at 5dpf. This supports literature showing LMX1b is required for the specification/differentiation of midbrain dopaminergic (mDa) neurones in zebrafish (Filippi 2007) and tetrapods (Smidt 2000). However, further TH-stained immunohistological sections of larval brains, particularly of the ventral midbrain where large dopaminergic populations develop in zebrafish (Rink 2002), are required to assess each paralogue's effects on dopaminergic neuronal development.

Fascinatingly, LMX1b-dependent neuronal specification/differentiation is also thought to be mediated via autophagy pathways; interactions of LMX1b with autophagy proteins ATG8 and LC3 are required for iPSC-derived human dopaminergic neurone differentiation and

maintenance (Moreno 2020). In mammals, LMX1b ablation in post-mitotic presynaptic mDa neurones is associated with downregulation of the autophagic-lysosomal pathway (ALP) and decreased expression of multiple autophagy proteins (including LC3, Beclin1, Lamp1) (Laguna 2015), which leads to neurodegeneration. Notably, neurodegeneration is reversed upon rescuing the ALP (Dehay 2010). Our model cannot explore the autophagy-mediated effects of post-mitotic LMX1b expression in mDa neurones because zebrafish do not express LMX1b in mature neurones (Filippi 2007). Nevertheless, these studies indicate that LMX1b is a critical mediator of autophagy in dopaminergic neurones, consequently autophagy defects may underlie the LMX1b-/- neuronal patterning abnormalities we observed.

Neurodevelopmental changes possibly persist into adulthood, with relevance to PD

Our behavioural investigations appear to suggest that reduction in LMX1bb expression has long-lasting effects on adult zebrafish behaviour. Although preliminary lab observations report LMX1b mutant behaviour seems generally normal, LMX1bb+/- and LMX1ba;LMX1bb+/- seem to demonstrate reduced bottom-dwelling and freezing behaviour in the novel environment test (see Fig.9). Fascinatingly, this corresponds to behavioural findings in zebrafish with depleted dopamine specifically in larval development (via transient TH-morpholino injection) (Formella 2012). In these fish, adult dopaminergic neurones/dopamine levels appeared unaffected. Parallels could be drawn between this scenario and LMX1b mutants; LMX1b is integral in larval dopaminergic neurone development), but is unexpressed in mature mDa neurones (Filippi 2007). Decreased freezing/bottom-dwelling behaviour is an anxiolytic behaviour typically displayed when dopamine levels decrease (Liu 2020, Lopez-Patino 2008). Our preliminary findings, combined with findings from Formella et al, may indicate that reduction in dopaminergic neurone signalling early in development leads to chronic changes to specific adult behaviours, whilst other behaviours are unaffected possibly due to compensation (Schwamborn 2018).

This has potential implications for PD modelling. There is increasing evidence that PD symptoms arise due to multiple ‘hits’ which damage midbrain dopaminergic neurones (Schwamborn 2018). These include neurodevelopmental, environmental and genetic defects (Sulzer 2007), which increase susceptibility to neurodegeneration later in life. Thus, it would be interesting to explore whether LMX1b-/- lines have increased susceptibility to neurodegeneration/dopaminergic neurodegeneration, and whether behaviour deteriorates at a different rate to wt. Sequential repetition of the novel environment experiment/other behavioural tests would be a first step.

Conclusions are tentative due to methodology limitations

The poor accuracy of manual eye, body and jaw length measurements could be vastly improved through automated analysis in both larvae and adults (Teixidó 2019). Jaw mounting issues resulted in angled confocal images, which caused jaw lengths to seem shorter than they would have been in horizontal sections. 3D rendering would alleviate this in future analysis. Additionally, Seg3D Sox9a intensity readings were hugely variable, and reliability could be increased by computing a standardised ROI panel into the Seg3D program, as well as normalising to non-Sox9a expression.

The usefulness of our TH-stained confocal images is limited because key dopaminergic populations exist more posterior to the brain region visible (Rink 2002). Additionally, conclusions from neuronal TH-staining and behavioural analysis remain tentative due to low sample sizes. Following the initial striking behavioural findings, increased sample size is required to determine whether freezing/bottom-dwelling behaviours are significantly ablated in LMX1bb mutants. Automated tracking software would be more reliable than stopwatch time-keeping and enable more aspects of alarm behaviour to be recorded efficiently. This could include the number of direction changes, % time spent in vertical tank quadrants and number of dives to bottom. (Kalueff 2013).

Lastly, post-mortem genotyping at 7dpf meant that 13/135 larvae had to be excluded from our analysis, because the genotype of all hetinX larvae which died prior to 7dpf was unknown. This limitation also caused larval survival analysis (Supp.Fig.1) to be inaccurate, as only the survival of LMX1ba homoinX (which had known genotype) could be properly tracked. Live genotyping of 3dpf larvae using caudal fin clips (Kosuta 2018) would alleviate this limitation, despite being more time-consuming.

Usefulness of our zebrafish LMX1b-/- model in studying skeletal and neuronal development

These results indicate our model may be more applicable for studying LMX1b's role in autophagy processes and neurodevelopment rather than skeletal development. A surprising lack of spinal and dorsoventral patterning larval defects are observed in comparison to in LMX1b mutant human patients. There is no tail curvature phenotype (a sign of abnormal patterning, Kanungo 2003) in mutant larvae (see Supp.Fig.4A), and prominent upper spine curvatures in LMX1bb-/- (see Supp.Fig.4B) are more likely a consequence of the generalised sickness phenotype than spinal defects. Normal mutant patterning could be because bone formation begins after 7dpf in zebrafish (Spoorendonk 2008). Alternatively, both paralogues might be expressed in the developing spine, so compensation by the other paralogue could

occur in each mutant line. A double knockout line would therefore confirm if LMX1ba and LMX1bb are both involved in dorsoventral and spinal patterning.

Double LMX1b knockout lines would additionally display greater resemblance to the mammalian condition and are therefore currently in development. Nevertheless, separately studying both differentially expressed paralogues in our current model enables different roles of LMX1b to be seen in separate models. This is advantageous when one specific phenotype leads to gross morphological changes/death (e.g. severe sickness of LMX1bb-/-) because other roles can be visualised in the opposing paralogue line (e.g. chondrogenesis in LMX1ba-/-). It is hoped that through studying the prominent neuronal and potentially autophagy-mediated larval mutant phenotypes in the zebrafish model, the cause of early lethality (which may be resulting in premature death of homozygote human mutant embryos) may be revealed. This highlights arguably the greatest advantage of the zebrafish model: external development of transparent embryos enables easy visualisation and assessment of the embryonic mutant form, which is unparalleled in mammalian embryonic models.

Conclusion

In conclusion, this project has allowed fascinating insight into the wide-ranging roles LMX1b might have across zebrafish development thereby supporting current literature that this transcription factor is more complex than simply regulating early patterning of skeletal systems. Nevertheless, refinements of genotyping procedure, accuracy of measurements and neuronal imaging/behavioural methodologies are required, in order to further investigate LMX1b's effects in autophagy-mediated developmental processes, and how resulting neurodevelopmental defects might persist into adult behaviour change.

References

Adams *et al.* (2000) 'The transcription factor Lmx1b maintains Wnt1 expression within the isthmic organizer', *Development (Cambridge, England)*, 127(9), pp. 1857–1867.

Aghajanian, P. and Mohan, S. (2018) 'The art of building bone: emerging role of chondrocyte-to-osteoblast transdifferentiation in endochondral ossification', *Bone Research*, 6, p. 19. doi: 10.1038/s41413-018-0021-z.

Aleström, P. *et al.* (2020) 'Zebrafish: Housing and husbandry recommendations', *Laboratory Animals*, 54(3), pp. 213–224. doi: 10.1177/0023677219869037.

Anderegg, A. *et al.* (2013) 'An Lmx1b-miR135a2 regulatory circuit modulates Wnt1/Wnt signaling and determines the size of the midbrain dopaminergic progenitor pool', *PLoS genetics*, 9(12), p. e1003973. doi: 10.1371/journal.pgen.1003973.

Arden, G. B. *et al.* (2011) 'Regression of early diabetic macular oedema is associated with prevention of dark adaptation', *Eye*, 25(12), pp. 1546–1554. doi: 10.1038/eye.2011.264.

Boyer, O. *et al.* (2013) 'LMX1B mutations cause hereditary FSGS without extrarenal involvement', *Journal of the American Society of Nephrology: JASN*, 24(8), pp. 1216–1222. doi: 10.1681/ASN.2013020171.

Chen, H. and Johnson, R. L. (2002) 'Interactions between dorsal-ventral patterning genes lmx1b, engrailed-1 and wnt-7a in the vertebrate limb', *The International Journal of Developmental Biology*, 46(7), pp. 937–941.

Chen, T. *et al.* (2018) 'Development of the Swimbladder Surfactant System and Biogenesis of Lysosome-Related Organelles Is Regulated by BLOS1 in Zebrafish', *Genetics*, 208(3), pp. 1131–1146. doi: 10.1534/genetics.117.300621.

Cosentino, C. C. *et al.* (2010) 'Intravenous Microinjections of Zebrafish Larvae to Study Acute Kidney Injury', *JoVE (Journal of Visualized Experiments)*, (42), p. e2079. doi: 10.3791/2079.

Dai, J.-X., Johnson, R. L. and Ding, Y.-Q. (2009) 'Manifold functions of the Nail-Patella Syndrome gene Lmx1b in vertebrate development', *Development, Growth & Differentiation*, 51(3), pp. 241–250. doi: https://doi.org/10.1111/j.1440-169X.2008.01083.x.

Dehay, B. *et al.* (2010) 'Pathogenic lysosomal depletion in Parkinson's disease', *The Journal of Neuroscience: The Official Journal of the Society for Neuroscience*, 30(37), pp. 12535–12544. doi: 10.1523/JNEUROSCI.1920-10.2010.

Dikic, I. and Elazar, Z. (2018) 'Mechanism and medical implications of mammalian autophagy', *Nature Reviews. Molecular Cell Biology*, 19(6), pp. 349–364. doi: 10.1038/s41580-018-0003-4.

Doucet-Beaupré, H., Ang, S.-L. and Lévesque, M. (2015) 'Cell fate determination, neuronal maintenance and disease state: The emerging role of transcription factors Lmx1a and Lmx1b', *FEBS Letters*, 589(24, Part A), pp. 3727–3738. doi: 10.1016/j.febslet.2015.10.020.

Dreyer, S. D. *et al.* (1998) 'Mutations in LMX1B cause abnormal skeletal patterning and renal dysplasia in nail patella syndrome', *Nature Genetics*, 19(1), pp. 47–50. doi: 10.1038/ng0598-47.

Filippi, A. *et al.* (2007) 'Expression and function of nr4a2, lmx1b, and pitx3in zebrafish dopaminergic and noradrenergic neuronal development', *BMC Developmental Biology*, 7(1), p. 135. doi: 10.1186/1471-213X-7-135

Filippi, A. *et al.* (2010) 'Expression of the paralogous tyrosine hydroxylase encoding genes th1 and th2 reveals the full complement of dopaminergic and noradrenergic neurons in zebrafish larval and juvenile brain', *The Journal of Comparative Neurology*, 518(4), pp. 423–438. doi: 10.1002/cne.22213.

Fontana, B. D. *et al.* (2018) 'The developing utility of zebrafish models of neurological and neuropsychiatric disorders: A critical review', *Experimental Neurology*, 299(Pt A), pp. 157–171. doi: 10.1016/j.expneurol.2017.10.004.

Formella, I. *et al.* (2012) 'Transient Knockdown of Tyrosine Hydroxylase during Development Has Persistent Effects on Behaviour in Adult Zebrafish (Danio rerio)', *PLoS ONE*. Edited by S. Strack, 7(8), p. e42482. doi: 10.1371/journal.pone.0042482.

Gistelinck, C. *et al.* (2016) 'Zebrafish Collagen Type I: Molecular and Biochemical Characterization of the Major Structural Protein in Bone and Skin', *Scientific Reports*, 6(1), p. 21540. doi: 10.1038/srep21540.

GraphPad Prism version 9.0.0 for Windows, GraphPad Software, San Diego, California USA, www.graphpad.com"

Guo, C. *et al.* (2007) 'Lmx1b is essential for Fgf8 and Wnt1 expression in the isthmic organizer during tectum and cerebellum development in mice', *Development*, 134(2), pp. 317–325. doi: 10.1242/dev.02745.

Hanke, N. *et al.* (2013) '"Zebrafishing" for novel genes relevant to the glomerular filtration barrier', *BioMed Research International*, 2013, p. 658270. doi: 10.1155/2013/658270.

Hobert, O. and Westphal, H. (2000) 'Functions of LIM-homeobox genes', *Trends in Genetics*, 16(2), pp. 75–83. doi: 10.1016/S0168-9525(99)01883-1.

Jászai, J. *et al.* (2003) 'Isthmus-to-midbrain transformation in the absence of midbrain-hindbrain organizer activity', *Development*, 130(26), pp. 6611–6623. doi: 10.1242/dev.00899

Jeon, H. and Im, G.-I. (2017) 'Autophagy in osteoarthritis', *Connective Tissue Research*, 58(6), pp. 497–508. doi: 10.1080/03008207.2016.1240790.

Jung, H. M. *et al.* (2017) 'Development of the larval lymphatic system in zebrafish', *Development (Cambridge, England)*, 144(11), pp. 2070–2081. doi: 10.1242/dev.145755.

Kalueff, A. V. *et al.* (2013) 'Towards a Comprehensive Catalog of Zebrafish Behavior 1.0 and Beyond', *Zebrafish*, 10(1), pp. 70–86. doi: 10.1089/zeb.2012.0861.

Kane SP. (2021) Sample Size Calculator.
ClinCalc: https://clincalc.com/stats/samplesize.aspx. Updated July 24, 2019. Accessed March 5, 2021.

Kanungo, J. *et al.* (2003) 'Gelsolin is a dorsalizing factor in zebrafish', *Proceedings of the National Academy of Sciences*, 100(6), pp. 3287–3292. doi: 10.1073/pnas.0634473100.

Kesavan, G. *et al.* (2017) 'CRISPR/Cas9-Mediated Zebrafish Knock-in as a Novel Strategy to Study Midbrain-Hindbrain Boundary Development', *Frontiers in Neuroanatomy*, 11. doi: 10.3389/fnana.2017.00052.

Khuansuwan, S. *et al.* (2019) 'A novel transgenic zebrafish line allows for in vivo quantification of autophagic activity in neurons', *Autophagy*, 15(8), pp. 1322–1332. doi: 10.1080/15548627.2019.1580511.

Kimmel, C. B. *et al.* (1995) 'Stages of embryonic development of the zebrafish', *Developmental Dynamics*, 203(3), pp. 253–310. doi: 10.1002/aja.1002030302.

Kosuta, C. *et al.* (2018) 'High-throughput DNA Extraction and Genotyping of 3dpf Zebrafish Larvae by Fin Clipping', *Journal of Visualized Experiments: JoVE*, (136). doi: 10.3791/58024.

Laguna, A. *et al.* (2015) 'Dopaminergic control of autophagic-lysosomal function implicates Lmx1b in Parkinson's disease', *Nature Neuroscience*, 18(6), pp. 826–835. doi: 10.1038/nn.4004.

Lichter, P. R. *et al.* (1997) 'Cosegregation of open-angle glaucoma and the nail-patella syndrome', *American Journal of Ophthalmology*, 124(4), pp. 506–515. doi: 10.1016/s0002-9394(14)70866-9.

Liu, S. *et al.* (2020) 'Carbofuran induces increased anxiety-like behaviors in female zebrafish (Danio rerio) through disturbing dopaminergic/norepinephrinergic system', *Chemosphere*, 253, p. 126635. doi: 10.1016/j.chemosphere.2020.126635.

López-Patiño, M. A. *et al.* (2008) 'Anxiogenic effects of cocaine withdrawal in zebrafish', *Physiology & Behavior*, 93(1–2), pp. 160–171. doi: 10.1016/j.physbeh.2007.08.013.

Lowry R. 2021 Freeman Halton Extension of Fisher's Exact Test. VasaarStats: http://vassarstats.net/fisher2x3.html Accessed March 5, 2021

Madeira. *et al.* (2019) 'The EMBL-EBI search and sequence analysis tools APIs in 2019.', *Nucleic Acids Research*, 47(W1), pp. W636–W641. doi: 10.1093/nar/gkz268

Manoli, M. and Driever, W. (2012) 'Fluorescence-activated cell sorting (FACS) of fluorescently tagged cells from zebrafish larvae for RNA isolation', *Cold Spring Harbor Protocols*, 2012(8). doi: 10.1101/pdb.prot069633.

Mark, M., Rijli, F. M. and Chambon, P. (1997) 'Homeobox Genes in Embryogenesis and Pathogenesis', *Pediatric Research*, 42(4), pp. 421–429. doi: 10.1203/00006450-199710000-00001.

Matthews, J. M. and Visvader, J. E. (2003) 'LIM-domain-binding protein 1: a multifunctional cofactor that interacts with diverse proteins', *EMBO reports*, 4(12), pp. 1132–1137. doi: 10.1038/sj.embor.7400030.

McIntosh, I. *et al.* (1997) 'Fine mapping of the nail-patella syndrome locus at 9q34', *American Journal of Human Genetics*, 60(1), pp. 133–142.

McMahon, C. *et al.* (2009) 'Lmx1b is essential for survival of periocular mesenchymal cells and influences Fgf-mediated retinal patterning in zebrafish', *Developmental biology*, 332(2), pp. 287–298. doi: 10.1016/j.ydbio.2009.05.577.

Minchin, J. E. N. *et al.* (2018) 'Deep phenotyping in zebrafish reveals genetic and diet-induced adiposity changes that may inform disease risk', *Journal of Lipid Research*, 59(8), pp. 1536–1545. doi: 10.1194/jlr.D084525.

Moreno, N. J. *et al.* (2020) 'LIR-dependent LMX1B-autophagy crosstalk shapes human midbrain dopaminergic neuronal resilience', *The Journal of cell biology*. Available at: ://research-ihttpsnformation.bris.ac.uk/en/publications/lir-dependent-lmx1b-autophagy-crosstalk-shapes-human-midbrain-dop (Accessed: 7 February 2021).

Morishita, H. *et al.* (2020) 'Autophagy Is Required for Maturation of Surfactant-Containing Lamellar Bodies in the Lung and Swim Bladder', *Cell Reports*, 33(10), p. 108477. doi: 10.1016/j.celrep.2020.108477.

Mork, L. and Crump, G. (2015) 'Zebrafish Craniofacial Development: A Window into Early Patterning', *Current Topics in Developmental Biology*, 115, pp. 235–269. doi: 10.1016/bs.ctdb.2015.07.001.

Moss, J. J., Hammond, C. L. and Lane, J. D. (2020) 'Zebrafish as a model to study autophagy and its role in skeletal development and disease', *Histochemistry and Cell Biology*, 154(5), pp. 549–564. doi: 10.1007/s00418-020-01917-2.

NCBI (2021) *National Center for Biotechnology Information*. Available at: http://www.ncbi.nlm.nih.gov/ (Accessed: 17 March 2021)

O'Hara, F. P. *et al.* (2005) 'Zebrafish Lmx1b.1 and Lmx1b.2 are required for maintenance of the isthmic organizer', *Development (Cambridge, England)*, 132(14), pp. 3163–3173. doi: 10.1242/dev.01898.

O'Sullivan, T. E. *et al.* (2016) 'Atg5 is essential for the development and survival of innate lymphocytes', *Cell reports*, 15(9), pp. 1910–1919. doi: 10.1016/j.celrep.2016.04.082.

Parichy, D. M. *et al.* (2009) 'Normal table of postembryonic zebrafish development: staging by externally visible anatomy of the living fish', *Developmental Dynamics: An Official Publication of the American Association of Anatomists*, 238(12), pp. 2975–3015. doi: 10.1002/dvdy.22113.

Postlethwait, J. *et al.* (1998) 'Chapter 8 The Zebrafish Genome', in Detrich, H. W., Westerfield, M., and Zon, L. I. (eds) *Methods in Cell Biology*. Academic Press (The Zebrafish: Genetics and Genomics), pp. 149–163. doi: 10.1016/S0091-679X(08)61898-1.

Resende, T. P., Andrade, R. P. and Palmeirim, I. (2014) 'Timing Embryo Segmentation: Dynamics and Regulatory Mechanisms of the Vertebrate Segmentation Clock', *BioMed Research International*, 2014, p. e718683. doi: 10.1155/2014/718683.

Richardson, R. *et al.* (2017) 'The zebrafish eye—a paradigm for investigating human ocular genetics', *Eye*, 31(1), pp. 68–86. doi: 10.1038/eye.2016.198.

Rink, E. and Wullimann, M. F. (2002) 'Development of the catecholaminergic system in the early zebrafish brain: an immunohistochemical study', *Developmental Brain Research*, 137(1), pp. 89–100. doi: 10.1016/S0165-3806(02)00354-1.

Rohr, C. *et al.* (2002) 'The LIM-homeodomain transcription factor Lmx1b plays a crucial role in podocytes', *The Journal of Clinical Investigation*, 109(8), pp. 1073–1082. doi: 10.1172/JCI13961.

Sackerman, J. *et al.* (2010) 'Zebrafish Behavior in Novel Environments: Effects of Acute Exposure to Anxiolytic Compounds and Choice of Danio rerio Line', *International Journal of Comparative Psychology*, 23(1), pp. 43–61.

Schindelin, J. *et al.* (2012) 'Fiji: an open-source platform for biological-image analysis', *Nature Methods*, 9(7), pp. 676–682. doi: 10.1038/nmeth.2019.

Schmidt, R., Strähle, U. and Scholpp, S. (2013) 'Neurogenesis in zebrafish – from embryo to adult', *Neural Development*, 8(1), p. 3. doi: 10.1186/1749-8104-8-3.

Schwamborn, J. C. (2018) 'Is Parkinson's Disease a Neurodevelopmental Disorder and Will Brain Organoids Help Us to Understand It?', *Stem Cells and Development*, 27(14), pp. 968–975. doi: 10.1089/scd.2017.0289.

Seg3D (2016) Seg3D: Volumetric Image Segmentation and Visualization. Scientific Computing and Imaging Institute, Download from: "http://www.seg3d.org"

Shiga, Y. *et al.* (2018) 'Genome-wide association study identifies seven novel susceptibility loci for primary open-angle glaucoma', *Human Molecular Genetics*, 27(8), pp. 1486–1496. doi: 10.1093/hmg/ddy053.

Shin, M. *et al.* (2016) 'Vegfc acts through ERK to induce sprouting and differentiation of trunk lymphatic progenitors', *Development*, 143(20), pp. 3785–3795. doi: 10.1242/dev.137901.

Singh, R. *et al.* (2009) 'Autophagy regulates lipid metabolism', *Nature*, 458(7242), pp. 1131–1135. doi: 10.1038/nature07976.

Smidt, M. P. *et al.* (2000) 'A second independent pathway for development of mesencephalic dopaminergic neurons requires Lmx1b', *Nature Neuroscience*, 3(4), pp. 337–341. doi: 10.1038/73902.

Snapgene Software (2021), from Insightful Science; available at snapgene.com

Spoorendonk, K. M. *et al.* (2008) 'Retinoic acid and Cyp26b1 are critical regulators of osteogenesis in the axial skeleton', *Development*, 135(22), pp. 3765–3774. doi: 10.1242/dev.024034.

Sulzer, D. (2007) 'Multiple hit hypotheses for dopamine neuron loss in Parkinson's disease', *Trends in Neurosciences*, 30(5), pp. 244–250. doi: 10.1016/j.tins.2007.03.009.

Teixidó, E. *et al.* (2019) 'Automated Morphological Feature Assessment for Zebrafish Embryo Developmental Toxicity Screens', *Toxicological Sciences*, 167(2), pp. 438–449. doi: 10.1093/toxsci/kfy250.

Uniprot (2021) UniProt: the universal protein knowledgebase in 2021 Nucleic Acids Res. 49:D1 (2021) Accessed March 15, 2021

Unpublished (2021) Moss, J Hammond Lab, Bristol University

Vaz, R., Hofmeister, W. and Lindstrand, A. (2019) 'Zebrafish Models of Neurodevelopmental Disorders: Limitations and Benefits of Current Tools and Techniques', *International Journal of Molecular Sciences*, 20(6), p. 1296. doi: 10.3390/ijms20061296.

Westerfield, M. (2007) THE ZEBRAFISH BOOK, 5th Edition; A guide for the laboratory use of zebrafish (Danio rerio), Eugene, University of Oregon Press. Paperback

Witzgall, R. (2017) 'Nail-patella syndrome', *Pflugers Archiv: European Journal of Physiology*, 469(7–8), pp. 927–936. doi: 10.1007/s00424-017-2013-z.

Wong, B. W. *et al.* (2017) 'The role of fatty acid β-oxidation in lymphangiogenesis', *Nature*, 542(7639), pp. 49–54. doi: 10.1038/nature21028.

Yan, Y.-L. *et al.* (2002) 'A zebrafish sox9 gene required for cartilage morphogenesis', *Development*, 129(21), pp. 5065–5079.

6. APPENDICES

6.1 Death of 20% LMX1ba-/- larvae at 2dpf.

Survival analysis indicates a highly significant difference ($p<0.0001$, Log-rank test) in survival rates of LMX1ba-/- (64% survival), LMX1bb-/- (89.5%) and sibs (100%). Lack of survival data past 7dpf means that the premature death of LMX1bb-/-, estimated 10-17dpf, is not shown. Additionally, survival data for LMX1ba/LMX1bb hetinx is only available for those that survive to at least 6dpf, due to post-mortem 7dpf genotyping. This limits validity of the analysis.

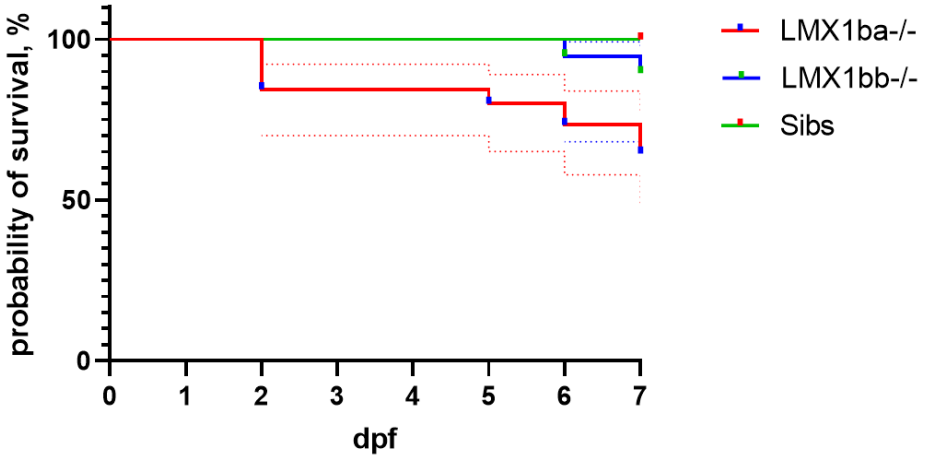

Supplementary Figure 1 *Kaplan Meier Survival Curve depicting survival of zebrafish larvae until 7dpf (n≥19)*

6.2 LMX1bb-/- display pronounced eye oedema from 5dpf.

Eye oedema is dramatically increased in LMX1bb-/-, with 16 out of 19 larvae developing eye oedema by 7dpf (see Supp.Fig2). Onset of eye oedema is typically 5dpf.

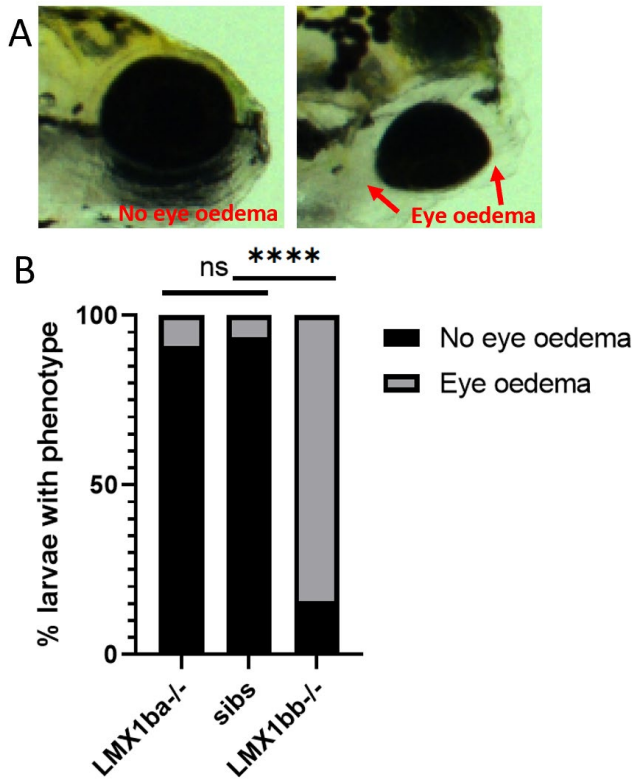

Supplementary Figure 2 *(A) Representative example of eye oedema phenotype, characterised as oedemic swelling in ocular region (red arrows). Shrinkage of eye diameter can be seen. (B) Graph showing % larvae which developed eye oedema (LMX1bb-/- vs sibs $p<0.0001$, Chi-squared test) ($n\geq19$)*

6.3 Equal percentage change in growth between LMX1ba-/- and wt jaws from 3-5dpf.

There is no significant difference in percentage growth from 3dpf to 5dpf in LMX1ba-/- and wt larval lower jaws (unpaired t-test), indicating that the effect of LMX1ba-/- on growth reduction occurs prior to 3dpf.

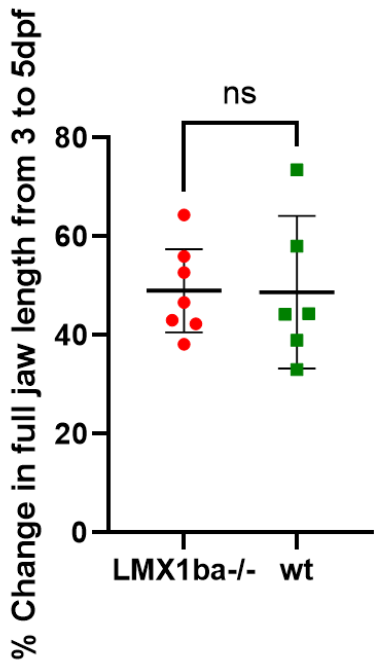

Supplementary Figure 3 *Graph comparing percentage change in jaw length between LMX1ba-/- and wt (n≥6).*

6.4 LMX1bb-/- show pronounced upper spine but not lower spine curvatures.

Supp.Fig.4C illustrates the incidence of tail curvatures does not increase in mutant larvae. LMX1bb-/- displayed slightly reduced incidence of tail bends compared to sibs. As seen in Supp.Fig4D, LMX1bb-/- display significantly increased incidence of upper spine bends by

7dpf.

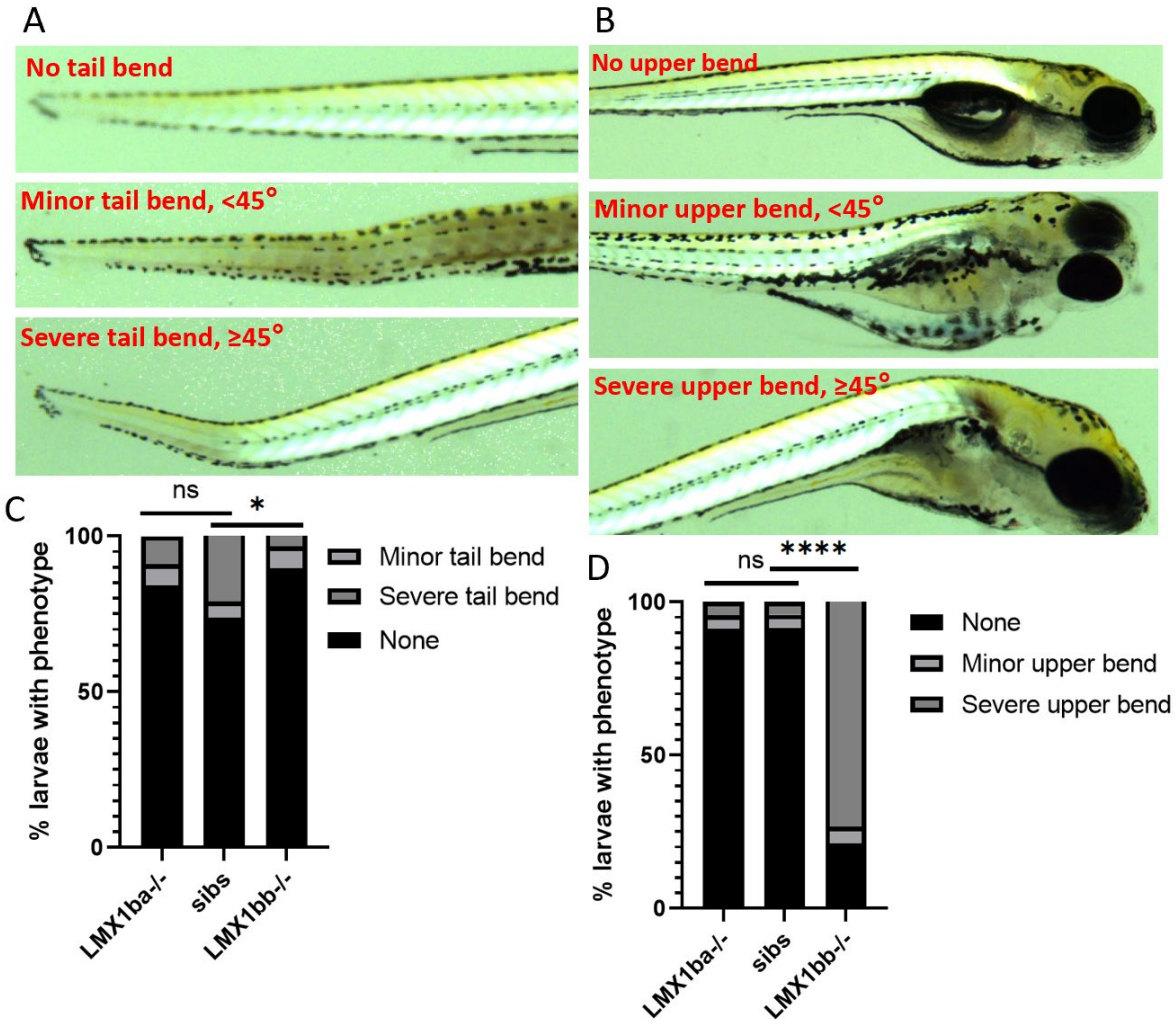

Supplementary Figure 4 *(A) Schematic displayed categories of tail bends, defined by angle of largest bend in notochord. Multiple bends were recorded as 'severe tail bend'. (B) Schematic displaying categories of upper bends, seen in region of the swim bladder/prior to the 1st somite (C) Graph comparing % of mutant and sib larvae with tail bends (LMX1ba-/- vs sibs p=0.052, LMX1bb-/- vs sibs p=0.498, Freeman-Halton Test) (n≥19). (D) Graph comparing % with upper bends (LMX1ba vs sibs p=1.0, LMX1bb vs sibs p<0.0001, Freeman-Halton Test) (n≥19).*